Electronic effects in scanning tunneling microscopy: Moiré pattern on a graphite surface

Zhao Y. Rong and Pieter Kuiper*
Physics Department, Brookhaven National Laboratory, Upton, New York 11973
(Received 27 July 1993)

We observed by scanning tunneling microscopy (STM) a hexagonal superlattice on graphite with a period of 66 Å. Direct measurement of the angle between lattice vectors confirmed that the superlattice is a Moiré pattern caused by a 2.1° rotation of the topmost (0001) plane with respect to the bulk. The STM corrugation of 2.6 Å is not due to physical buckling, but to differences in electronic structure between *AA*-stacked, normal *AB*-stacked, and rhombohedral *CAB*-stacked graphite. The high tunneling current of *AA*-stacked regions is in agreement with the high density of states at the Fermi level calculated for *AA* graphite. The Moiré pattern changes, both the amplitude and the shape, with bias voltage. The observation provides a basis for a comparative study of surface electronic structures with different subsurface layer configuration, which is a vital test of our understanding of STM.

INTRODUCTION

Normal graphite, which has a Bernal structure where the layers of a hexagonal network of carbon atoms are stacked in an *ABAB* fashion, has been studied extensively by scanning tunneling microscopy (STM). The easily obtained atomic images have two well-known anomalies, i.e., the asymmetry between neighboring atoms and giant (>1 Å) vertical corrugations. These interesting anomalies had initiated a long-lasting debate on what role the following are playing in STM imaging: (1) electronic structure effects,[1] (2) tip electronic orbitals,[2] (3) tip-sample interactions,[3] and (4) subsurface layer influences.[4,5] One interesting experiment that will help in understanding these issues is to alter the graphite stacking sequence. Rhombohedral graphite (*ABCABC* stacked) can be found in crystalline graphite as a minority phase. It has been identified by Snyder *et al.* in STM images of dislocation-network structures.[6] The simple hexagonal graphite (*AAA* stacked) has not been observed in crystalline graphite, but has been studied by Kelty and Lieber in graphite intercalation complexes.[7] However a comparative STM study of all the three stacking configurations has not been made. Recently, one type of superlattice on graphite surface has been reported repeatedly.[8–16] These are centered hexagonal lattices with periodicity ranging from 17 to 440 Å. They extend over thousands of Å and terminate by sharp boundaries. Kuwabara, Clarke, and Smith[11] suggested that the superlattice may be rotational Moiré patterns, where the topmost (0001) sheet is rotated by a small angle with respect to the substrate. This was recently confirmed by Xhie *et al.*[16] by imaging the atomic lattice vectors on both sides of a boundary which separates the superlattice from the normal region. In this paper we will prove that these graphite superlattices provide a unique system which makes possible the comparative study of three stacking structures.

In this paper we provide STM images of superlattice on graphite. Further evidence of the top layer rotation came from the direct measurement of the second-layer atomic lattice vector. The rotation leads to a Moiré pattern of regions with different stacking: *AAB*, *BAB*, and *CAB* nested in a centered hexagonal pattern. We will try to identify these different regions in our STM images. We relate these data to recent band-structure calculations on simple hexagonal *AAA*-stacked graphite and rhombohedral (*CAB* stacked) graphite,[17] and on the normal hexagonal *AB*-stacked Bernal structure. The basic features, e.g., the larger (~2.6 Å) corrugation, are understood in term of surface density of states (DOS).

EXPERIMENT

The highly oriented pyrolitic graphite (HOPG) sample (Union Carbide, grade ZYH) is prepared by cleaving with adhesive tape in air. The STM is constructed based on Pan's design,[18] with a shear piezoactivator for the autoapproach of the tip, and controlled by a control unit (Model STM 100) from RHK Technology. The tip is mechanically cut from Pt90/Ir10 wire. All images were obtained in constant-current mode in air ambient conditions.

RESULTS

A hexagonal superlattice with a period of 66 Å was found on part of the graphite sample in our STM measurement (the lower part of Fig. 1). A boundary, resembling a string of beads, of more than one micrometer long separates the HOPG (0001) cleavage plane into a normal graphite region (the top part of Fig. 1) and a superlattice region, and it terminates on the right side of the image with a step of three atomic layers. The region with the superlattice is interrupted by a strip about 1000 Å wide. On both sides of this strip are edges about 3.5 Å high, which represent one atomic layer. Apparently, a 1000-Å-wide monolayer has been stripped away from the middle of this region, exposing a second layer without a superlattice. The superlattice is rotated $\approx 30°$ with respect to the atomic orientation. Previous studies have suggested that this superstructure was due to a Moiré pattern caused by a rotated top layer. Therefore we looked at the rotation of the atomic corrugation in the superstructure layer with respect to the exposed second layer and the normal

0163-1829/93/48(23)/17427(5)/$06.00

region across the boundary. We found a $2.7\pm0.7°$ mismatch in orientation with respect to both of these regions. The height difference across the beadlike boundary is smaller than 0.5 Å. Therefore, this boundary represents a twin boundary. It was not possible to obtain stable atomically resolved images at this boundary. The z contrast of the superstructure is uniform throughout.

The period of a Moiré pattern caused by a relative rotation θ is given by

$$D = d/[2\times\sin(\theta/2)] \approx d/\theta\ , \quad \phi = 30° - \theta/2\ , \qquad (1)$$

where D and ϕ are the periodicity and orientation of the Moiré pattern, and $d = 2.45$ Å is the lattice constant of graphite.[11] If we set the ratio of the lattice constant to the period of the superlattice in Eq. (1), we find $\theta = 2.1°$. The agreement of θ and ϕ with the directly measured angle and orientation of the superlattice confirms that the superlattice is a rotation-induced Moiré pattern.

Figure 2(a) shows a more detailed view of the superlattice in which the atomic structure is also visible. The image is taken in the constant-current mode with a set tunneling current of 5 nA, and a tip bias voltage of 72 mV. The scan speed is 0.1 s/line. The image shows bright peaks in a centered-hexagonal lattice, each surrounded by a hexagonal ring of six grayish valleys (similar to those reported by Kuwabara, Clarke, and Smith[11]). Further magnified images show that the a-β-site asymmetry $[A \equiv (z_\beta - z_a)/(z_\beta + z_a)]$ in the grayish regions is ~ 0.56 (equal to the normal region), while in the white region it is ~ 0.17. Figure 2(b) is the cross section along the line indicated in Fig. 2(a). It shows corrugations of both the superlattice and atomic lattice. For the superlattice, the higher peak is 2.6 Å, and the lower one is 0.8 Å. There is a slight difference between two valleys (0.3 Å measured from an average of scans over a larger area). The atomic corrugation is 0.6 Å.

When we increase the bias voltage to 535 meV, the STM image shows a superlattice with the same periodicity as in Fig. 2(a), but the six-valley structure which surrounded every brightest peak in Fig. 2(a) has been replaced by a triangular pattern (similar to those reported

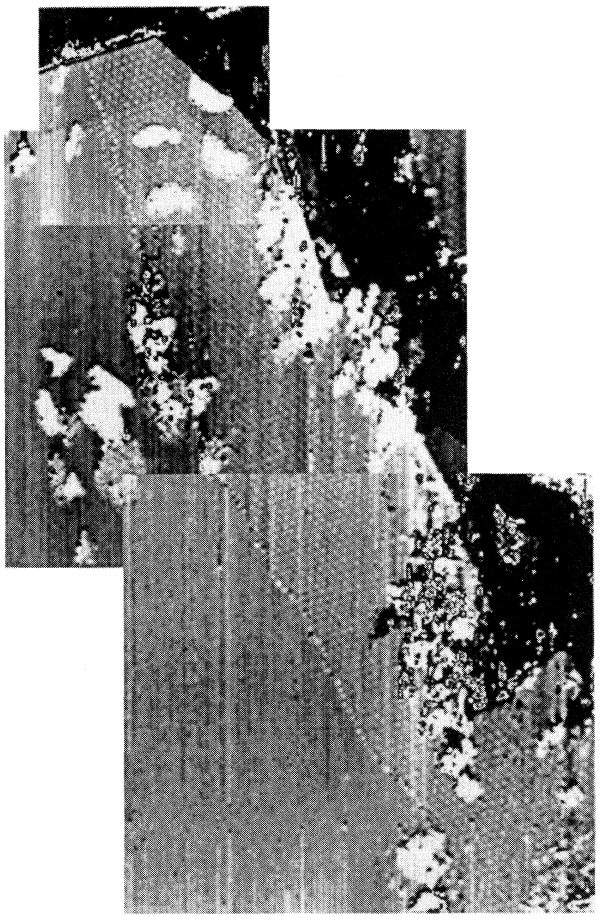

FIG. 1. Large-scale images of the superlattice (lower right) and its boundary with normal graphite region (upper left). These images are taken with set current 2.3 nA and tip bias 490 mV. The size of the left bottom square is a 4000×4000 Å^2. The gray-scale range is 3 Å. The hexagonal superstructure has a periodicity of 65.8 Å.

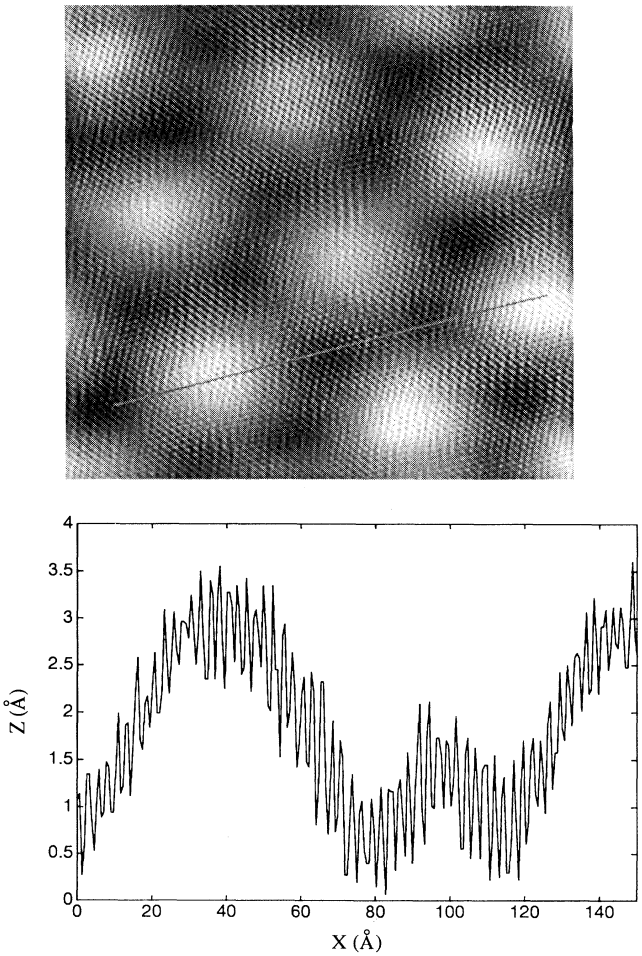

FIG. 2. (a) A closeup view of the superlattice on which graphite atoms are resolved. The image is taken with set current 5.6 nA, tip bias 72 mV, and scan size 202×202 Å^2. The image is low pass filtered. (b) A cross section along the direction indicated by the line in (a).

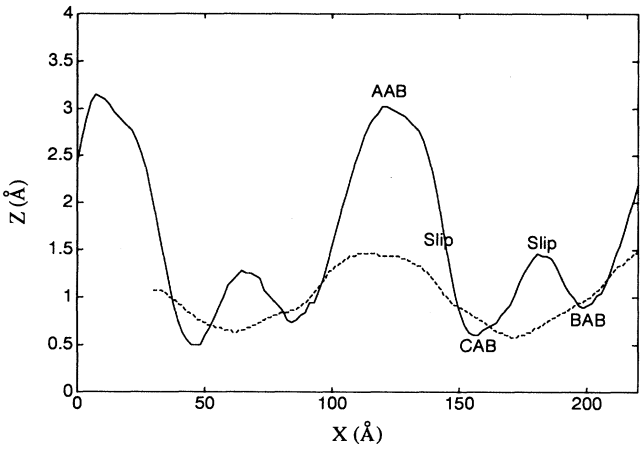

FIG. 3. Cross-section plots along the same direction as of Fig. 2(b). The solid curve is with tip bias 72 mV, and the dashed curve is with tip bias 535 mV.

by Xhie *et al.*[16] and by Liu, Chang, and Bard[12]). Figure 3 is a comparison of two scan lines scanned at 72 (solid) and 535 meV (dashed), respectively, along the same direction as that of Fig. 2(b). We can see clearly that there are two major changes in the dashed line as compared to the solid line: (1) the Moiré pattern corrugation is reduced by a factor of 3; and (2) the lower peak has disappeared. At 535-mV bias, the atomic corrugation is 0.4 Å (not shown).

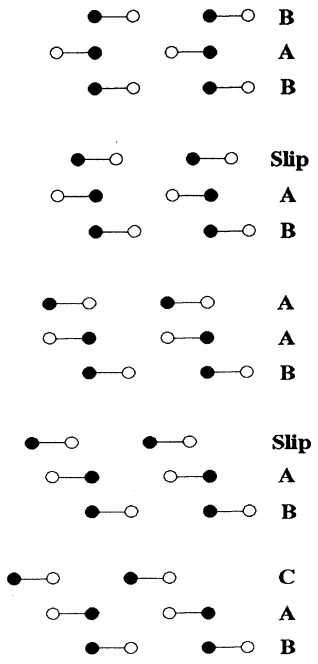

FIG. 4. Sliding the top graphite layer by different distances generates different stacking structures. Black circles and white circles are a- and β-site atoms of BAB stacking, respectively; these do not apply to other stacking sequences.

DISCUSSION

Direct measurement of the atomic lattice vector of the second layer further confirms that the hexagonal superlattice imaged on graphite is a rotational Moiré pattern. The observed single-layer rotation, twin boundary termination, and undisturbed Moiré pattern on both sides of a cleavage strip suggests that it is an epitaxial rotation in the growing process of graphite. For our sample, a hexagonal graphite sheet is rotated 2.1° with respect to the underlying $ABAB$-stacked graphite. Therefore the local atomic configuration of subsurface layers can simply be determined by the Moiré pattern geometry. One can visualize this Moiré pattern by overlaying two identical hexagonal patterns on transparencies and rotating one with respect to the other. Good diagrams can be found in Refs. 13 and 16. The periodicity can be understood by continually shifting the top graphite layer against the sublayers, which gives us a periodicity in the following order: BAB-slipped–AAB-slipped–CAB-slipped–BAB, and so on (see Fig. 4), where the slipped region is defined as the top layer slipped by half of the C-C bond distance.

Thus there are three kinds of regions with high rotational symmetry: BAB, AAB, and CAB. Our aim in this paper is to identify the high-symmetry points in the Moiré pattern with these structures. There are a number of different arguments, and we will see that they all point in the same direction.

The first argument is as follows: It is reasonable to assume that the third layer has less influence on the image than the second layer. Because one expects a larger difference between AAB and BAB stacking than between CAB and BAB stacking, we assume that the high-current symmetry points are due to the AAB-stacked regions, and that the lower-current regions are due to BAB and CAB stacking.

The second argument is that the asymmetry between a and β sites in normal AB-stacked graphite should be greatly reduced in the AAB-stacked region. It is consistent with this assignment that the asymmetry of neighboring atoms is stronger in the grayish BAB or CAB regions than in the white AAB regions.

The third argument is the higher density of states calculated for AAA graphite, upon which we will elaborate in detail below.

Based on arguments listed above, we have assigned the stacking along the curve of Fig. 3. So far we cannot identify between BAB and CAB regions. We chose to assign the CAB region as the deepest valley, and a justification based on the calculated DOS will be given below. Therefore, the largest corrugation along the curve (2.6 Å) is from AAB to CAB. The slipped region is peaked by 0.8 Å between the BAB and CAB valleys. A much smaller contrast between BAB and CAB is 0.3 Å.

The origin of STM corrugation is a matter of debate. The first interpretation of this STM Moiré pattern would be that this corrugation reflects a physical buckling of the top layer. It appeals to a simple rigid-sphere intuition that the interlayer separation of AA-stacked graphite would be larger than that of AB-stacked graphite, and it

is even conceivable that the AA stacking would be repulsive. But according to *ab initio* calculations, hypothetical graphite with AA stacking has virtually the same interlayer spacing as AB-stacked graphite, 3.3 Å.[19] It is less surprising that a diffraction study of CAB-stacked orthorhombic graphite also has the same interlayer spacing.[20] Furthermore, although it does not require much energy to roll up a stiff sheet (like graphite or paper) in one direction to a cylinder or a cone, it requires much more to cause a buckling deformation where the sheet is alternately expanded and compressed. Thus we conclude that the corrugation does not represent the real atomic displacement in that third dimension. The same reasoning also suggests that misorientation between graphite sheets will not cause in-plane atomic distortion. A claim has been made that the superstructure is due to a dislocation network,[15] but our data [Fig. 2(a)] do not confirm that.

The compressibility of bulk AAA graphite along the c axis is calculated to be six times weaker than that of AB graphite.[19] This suggests the possibility that our Moiré pattern may be due to a difference in the deformability of the different stacking structures. However, the fact that our sample is a patch of rotated graphite monolayer lying 3.3 Å above a common substrate, as proved by our measurements, suggests that the deformability effect is much smaller than 2.6 Å.

We believe that the corrugation must be due mainly to electronic structure. A well-known illustration of STM corrugations not related to atomic displacements is the α-β-site asymmetry of graphite. Graphite consists of (0001) basal planes of a hexagonal arrangement of carbon atoms, each bound to three nearest neighbors. These layers are stacked in an $ABAB$ sequence, so that there are two inequivalent carbon sites: α sites that are located between two neighbors in the layers directly above and below along the c axis, and β sites that are located between the empty centers of neighboring hexagons. Surpisingly, STM can detect a strong symmetry in the z corrugation between these two inequivalent carbon sites in the surface layer. This is not due to a real buckling of the surface layer. There is also no difference in calculated charge clouds for α and β surface sites. Thus, despite the weak coupling and large distances between the planes, the underlying layers have a large effect. Tománek *et al.*[4] link this asymmetry to the site-dependent nature of the density of states. They reason that the flatband that crosses the Fermi level is due to the small overlap of the π_z orbitals on β sites (the sites without a close neighbor in the next layers), that this narrow band is responsible for the density of states at the Fermi level, and that therefore the density of states on β sites is high, which makes them show up much more strongly in the STM image than the α sites. (Other factors may also contribute to the asymmetry, as suggested by recent experiments.[5,21])

The STM image of a Moiré pattern can also be checked by a band-structure calculation based on the Tersoff and Hamann formalism.[22] This is especially true in our case, where we have a large lattice constant so that the s-tip model can be readily applied.[2] A simple comparison with available theoretical calculations can be made. A recent band-structure calculation[17] of hypothetical AA-stacked graphite gives a density of states of 0.0085 states/eV. Surprisingly, this is three times higher than that of normal AB or CAB-stacked rhombohedral graphite, which is opposite to what one would expect from an analogy to α sites. (In AA stacking, all atoms have a close neighbor in the next layer.) This would explain the apparently high-z values at AAB-stacked graphite in our data. The computed DOS of AB-stacked graphite is 0.0033 states/eV (0.0056 for β sites and 0.0011 for α sites). For CAB-stacked graphite, it is 0.0021 states/eV. It seems reasonable to assign the deepest valley, i.e., the darkest color pattern in the picture, to the CAB-stacked region, and the other valley to the BAB-stacked region. Then the ratio of corrugation from AA to CAB vs the corrugation from BAB to CAB can be calculated from their respective DOS values, which leads to a ratio of 5.3, a bit smaller than the result (8.3) from Fig. 3 (solid curve).

We should point out that our designations of CAB as the darkest region, and BAB as the grayish region, are in conflict with reported STM images of a mixed rhombohedral-normal graphite sample.[6] The contrast between the CAB and BAB regions was inverted compared to the bulk DOS calculation. But in that case the elastic effect might be different for regions, something that does not apply to our work. In our case, elastic effects may enhance the amplitude of corrugation, but do not change the contrast between regions of different type. We conclude that the DOS at E_F can explain the large-z corrugation, but the small contrast between CAB and BAB, as well as the slipped peak, should be treated with more specified calculation.

The amplitude of the atomic corrugation of graphite is known to be voltage dependent, which can be understood as an elastic effect.[3] Especially, since all the images presented here were taken in the air, a contamination layer on the sample surface is expected. However, our STM images show a stronger voltage dependence of the superlattice corrugation than the atomic, which may suggest that the electronic effect is also important. The weakening of superlattice amplitude with increasing bias voltage is consistent with the understanding that the interlayer influence is only important near the Fermi level.[17] The disappearance of the slipped peak at higher bias voltage can also be found out by comparing reported images of Fig. 1(b) of Ref. 11 ($V_{\text{bias}}=75$ mV) and Fig. 2(a) of Ref. 12 ($V_{\text{bias}}=200$ mV). Our result shows that the change is not due to the difference in samples, but rather to a difference in the I-V characteristics of different stacking structures. This is especially prominent between regions with triangular symmetry (e.g., AAB, BAB, and CAB) and regions without (e.g., the slipped configuration).

Our assignment of local stacking is different from Ref. 16, where the AA-stacked region is assigned to the deepest valley. The reasoning in Ref. 16 is based on the surface-atom location relative to AB-stacked crystal: atoms above hole sites give the highest intensity, atoms above α sites give the second-highest intensity, and atoms above β sites give the minimum intensity. We believe that the local crystal structure of the topmost layers is crucial in a DOS consideration.

CONCLUSIONS

We have observed by STM a hexagonal superlattice with a period 66 Å on HOPG. This is a Moiré pattern cause by a 2.1° rotation of the top layer with respect to the bulk. This is confirmed by our direct measurement of the atomic lattice vector of the second atomic layer. We have assigned the high-symmetry point of the superlattice to different stacking sequences. *AAB*-stacked regions in the Moiré pattern are found brighter than *BAB* and *CAB* regions, and our assignment is different from what has been reported. The STM contrast of Moiré pattern comes from the strong influence of subsurface layers on surface electronic structures near the Fermi level. The *AA*-stacking structure shows a high tunneling current, and hence a high DOS, which is consistent with the recent band-structure calculation of *AA*-stacked graphite. The Moiré pattern changes its shape while the bias voltage changes, which indicates different *I-V* characteristics for different stacking configurations. A STM scattering calculation[23] of this sample system may help to understand further this frequently reported defect on graphite.

ACKNOWLEDGMENTS

We thank Leonid Rokhinson for help in STM instrumentation and Mayer Landau for suggested improvements in the manuscript. This work was supported by the U.S. Department of Energy under Contract No. DE-AC02-76CH00016. One of us (Z.Y.R.) would like to acknowledge the support from Laboratory Directed Research Funds. This work was also partially supported by the Air Force Office of Scienctific Research, Grant No. AFOSR Grant No. F49620-92-J-0358.

---

*Present address: Department of Physics, Uppsala University, Box 530 S-751 21, Uppsala, Sweden.

[1]J. Tersoff, Phys. Rev. Lett. **57**, 440 (1986).
[2]J. Tersoff, Phys. Rev. B **41**, 1235 (1990); J. Tersoff and N. D. Lang, Phys. Rev. Lett. **65**, 1132 (1990).
[3]J. M. Soler, A. M. Baro, N. Garcia, and H. Rohrer, Phys. Rev. Lett. **57**, 444 (1986).
[4]D. Tománek, S.G. Louie, H. J. Mamin, D.W. Abraham, E. Ganz, R. E. Thomson, and J. Clarke, Phys. Rev. B **35**, 7790 (1987).
[5]S. Gwo and C. K. Shih, Phys. Rev. B **47**, 13 059 (1993).
[6]S. R. Snyder, T. Foecke, H. S. White, and W. W. Gerberich, J. Mater. Res. **7**, 341 (1992); S. R. Snyder, W. W. Gerberich, and H. S. White, Phys. Rev. B **47**, 10 823 (1993).
[7]S. P. Kelty and C. M. Lieber, Phys. Rev. B **40**, 5856 (1989).
[8]T. Hashizume, I. Kamiya, Y. Hasegawa, N. Sano, T. Sakurai, and H. W. Pickering, J. Microsc. **152**, 347 (1988).
[9]J. W. Lyding, J. S. Hubacek, G. Gammie, S. Skala, R. Brockenbrough, J. R. Shapley, and M. P. Keles, J. Vac. Sci. Technol. A **6**, 363 (1988).
[10]V. Elings and F. Wudl, J. Vac. Sci. Technol. A **6**, 412 (1988).
[11]M. Kuwabara, D. R. Clarke, and D. A. Smith, Appl. Phys. Lett. **56**, 2396 (1990).
[12]C.-Y. Liu, H. Chang, and A. J. Bard, Langmuir **7**, 1138 (1991).
[13]P. I. Oden, T. Thudnat, L. A. Nagahara, S. M. Lindsay, G. B. Adams, and O. F. Sankey, Surf. Sci. Lett. **254**, L454 (1991).
[14]J. E. Buckley, J. L. Wragg, H. W. White, A. Bruckdorfer, and D. L. Worcester, J. Vac. Sci. Technol. B **9**, 1079 (1991).
[15]J. Gabarz, E. Lacaze, G. Faivre, S. Gauther, and M. Schott, Philos. Mag. A **65**, 853 (1992).
[16]J. Xhie, K. Sattler, M. Ge, and N. Venkateswaran, Phys. Rev. B **47**, 15 835 (1993).
[17]J.-C. Charlier, J.-P. Michenaud, and Ph. Lambin, Phys. Rev. B **46**, 4540 (1992).
[18]S. H. Pan, S. Behler, M. Bernasconi, and H.-J. Güntherodt, Bull. APS **37**, 167 (1992).
[19]J.-C. Charlier, J.-P. Michenaud, and X. Gonze, Phys. Rev. B **46**, 4531 (1992).
[20]H. Lipson and A. R. Stokes, Proc. R. Soc. London, Ser. A **181**, 101 (1942).
[21]T. A. Land, T. Michely, R. J. Behm, J. C. Hemminger, and G. Comsa, Surf. Sci. **264**, 261 (1992).
[22]J. Tersoff and D. R. Hamann, Phys. Rev. B **31**, 805 (1985).
[23]P. Sauter and C. Joachim, Ultramicroscopy **42-44**, 115 (1992).

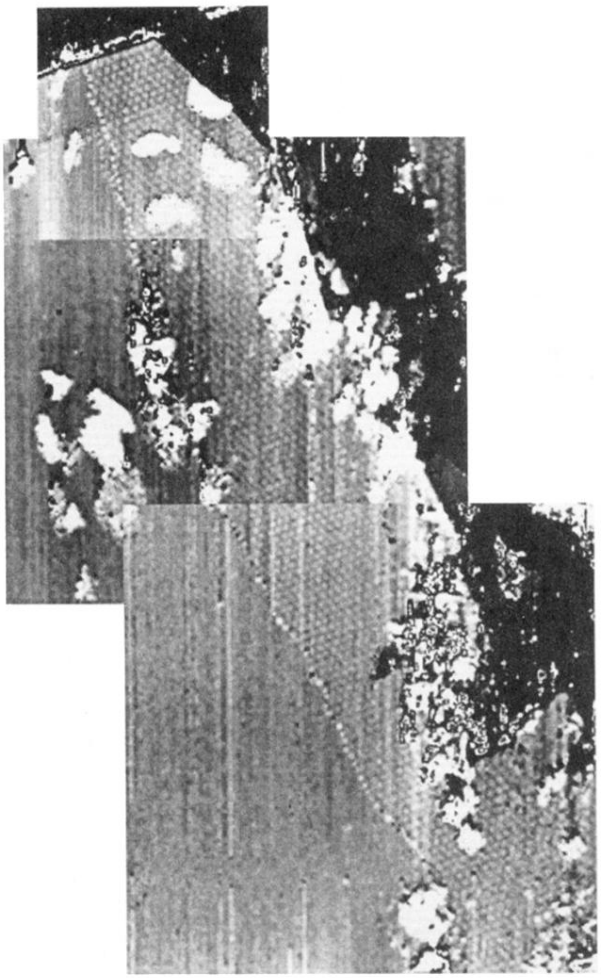

FIG. 1. Large-scale images of the superlattice (lower right) and its boundary with normal graphite region (upper left). These images are taken with set current 2.3 nA and tip bias 490 mV. The size of the left bottom square is a 4000×4000 Å^2. The gray-scale range is 3 Å. The hexagonal superstructure has a periodicity of 65.8 Å.

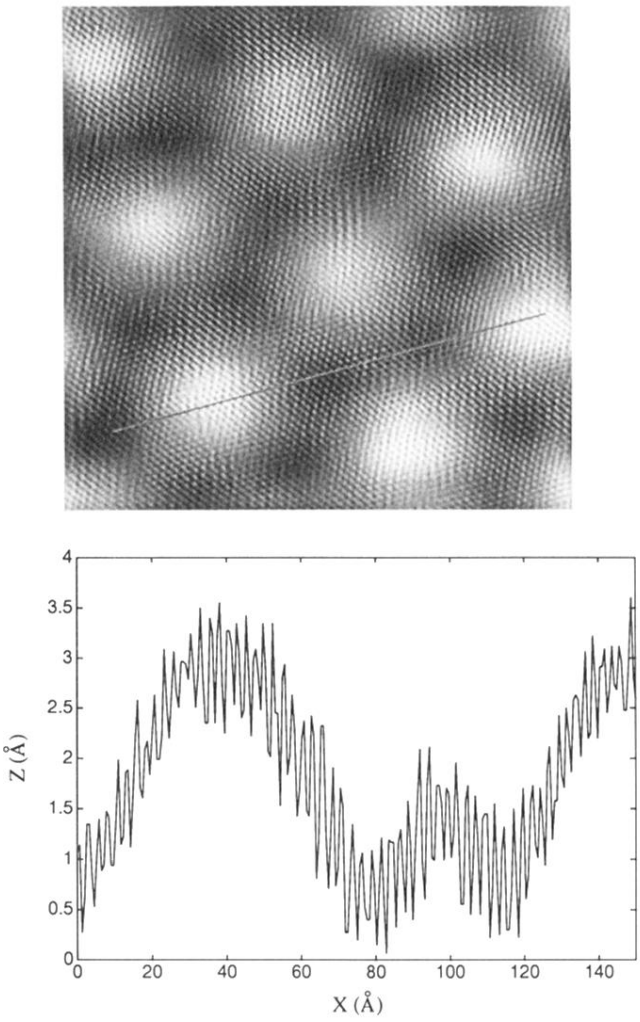

FIG. 2. (a) A closeup view of the superlattice on which graphite atoms are resolved. The image is taken with set current 5.6 nA, tip bias 72 mV, and scan size 202×202 Å^2. The image is low pass filtered. (b) A cross section along the direction indicated by the line in (a).